ACS Macro Letters

Letter

pubs.acs.org/macroletters

Innovative Approach to Rapid Growth of Highly Clay-Filled Coatings on Porous Polyurethane Foam

Yeon Seok Kim, Richard Harris, and Rick Davis*

Engineering Laboratory, National Institute of Standards and Technology, 100 Bureau Drive MS-8665, Gaithersburg, Maryland 20899-8665, United States

ABSTRACT: An innovative twist to fabricating layer-by-layer coatings resulted in transparent, high-content clay coatings on porous polyurethane foam. The addition of an anionic poly(acrylic acid) (PAA) monolayer between anionic clay and cationic branched-polyethylenimine (PEI) monolayers resulted in a trilayer nanocomposite structure with an order of magnitude thicker coating using 40% less monolayers than the conventional bilayer approach. The eight trilayer system thoroughly coated all internal and external surfaces of the porous polyurethane foam, creating a clay brick wall barrier that reduced the foam flammability by as much as 17% of the peak heat release rate and 21% of the total burn time. Though the flammability reduction is comparable to common commercial fire retardant polyurethane foam, the clay is used at a 50% lower amount and may be a greener solution as many of the commercial fire retardants (e.g., halogen bases) have potential environmental and health concerns.

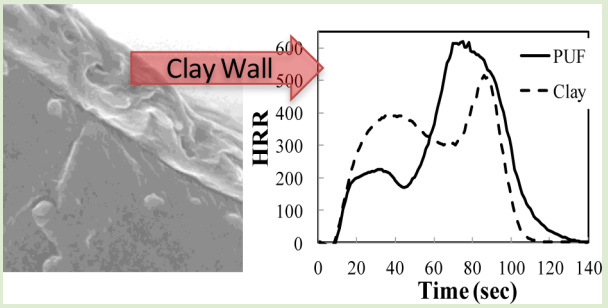

Layer-by-layer (LbL) assembly is a method to fabricate multifunctional, multilayer thin films on the surface of a substrate.[1,2] LbL films are generally fabricated by alternate deposition of an anionic monolayer and cationic monolayer (collectively called a bilayer (BL)) onto a substrate and repeating this process until the desired number of BLs are deposited to provide a film with the required characteristics. The layers are held together through electrostatic,[3] van der Waals,[4] H-bonding,[5] and in some cases covalent bonds.[6] LbL films have a wide variety of properties and applications (e.g., as a conducting film,[7] antireflection film,[8] and oxygen barrier[9] for biomedical[10] and sensor applications[11]) where the substrates have a simple architecture and nearly two-dimensional geometry.

In the last two years, researchers have demonstrated that LbL films can be fabricated on the surface of complex substrates to impart a reduction in flammability.[12,13] For example, clay-filled LbL coatings on cotton fabric resulted in a significant retention of fabric like char after conducting vertical burn tests, and there was no (or less) ember afterglow when the flame was removed.[13] Previously, we reported that a four BL (4BL) carbon nanofiber (CNF)-filled LbL coating on polyurethane foam (PUF) reduced the PUF peak heat release rate (PHRR) by 40%, which is a 100−1100% greater reduction than achieved with 17 different fire retardants commercially used in PUF.[12] Potential drawbacks to using CNF are the black color of the finished product and the possibility that CNF may have negative environmental, health, and safety characteristics.

Montmorillonite clay (MMT) is a natural material which has been shown to reduce the flammability of materials[14−18] through the enhancement or generation of an intumescent char protective layer on the surface of the substrate. Clay has also been shown to work well in LbL process without modification because of its inherently weak anionic charge and good water dispersion at low concentrations. The light gray to white color of clay generally results in only a slightly off-white discoloration when incorporated into a polymer and often forms transparent films even when highly aggregated as in LbL fabricated films.[19,20] The proposed mechanism for the formation of a clay protective char is the volatilization of polymer pyrolysis products that generate an intumescent coating containing a high concentration of clay at the surface. Critical to this process is a polymer that can form an intumescent char, a sufficient amount of the polymer to form an intumescent char, and the clay at the surface to prevent the transport of heat in the polymer and volatiles out of the substrate. The rate-limiting step in char formation is the concentration of the clay at the surface that results from polymer pyrolysis. LbL coatings may accelerate the formation of the protective char because the clay is already concentrated at the surface (in the coating) without the polymer pyrolyzing. However, to avoid the foam from participating in the combustion and for this technology to be commercially viable, the coating must exhibit rapid film growth with a high clay concentration to result in a sufficiently thick coating using the minimum number of layers. Growth behavior of clay-filled LbL coating has been extensively studied, and most studies show a linear growth when clay platelets were deposited with one polymer.[13,21−23] Podsiadlo et al.[24] showed that a quad-layer system (PEI/PAA/PEI/MMT) can exhibit exponential growth with a coating thickness of 200 μm after 200 pairs of layers. This quad-layer approach results in coatings with less than 10 mass % of clay,

Received: March 1, 2012
Accepted: June 11, 2012
Published: June 15, 2012

which is at least 5 times too low to be an adequate fire retardant coating.

Reported here is a trilayer (TL) system (PEI/MMT/PAA) that exhibits a more rapid exponential growth pattern using less layers on porous PUF. Discussed are the LbL methodologies to fabricate sodium MMT clay-filled coatings on PUF, the benefits of using a novel TL rather than the conventional BL assembly approach, characterization of these coatings (e.g., scanning electron microscopy (SEM)), and an assessment of flammability reduction caused by the coatings (e.g., cone calorimetry).

A single BL deposition unit is constructed of two monolayers; a polyethylenimine (PEI; cationic) and a MMT (anionic) monolayer. A single TL deposition unit is constructed of three monolayers; a PEI, a MMT, and a poly(acrylic acid) (PAA; anionic) monolayer. This additional monolayer of PAA significantly increased the coating growth rate and MMT concentration in the coating. Though both MMT and PAA are anionic, growth still occurs because of the hydrogen bonding of the PAA carbonyls with the MMT hydroxyl groups.[25] The mass of the BL coating grew linearly through 15 deposition units (mass measured by quartz crystal microbalance (QCM), Figure 1). At less than 5 deposition units, the TL coating exhibited a

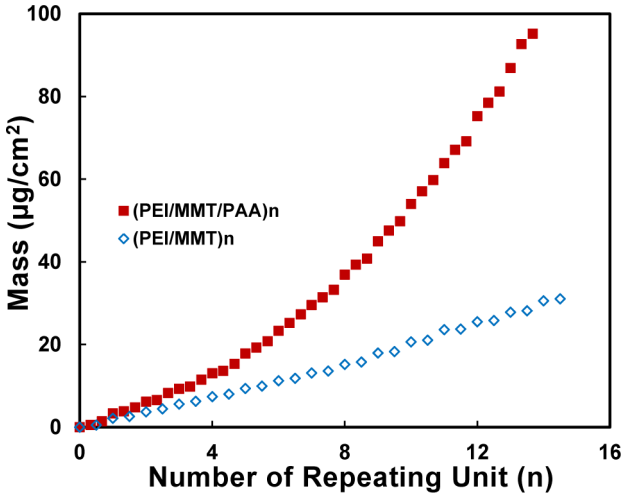

Figure 1. Mass (measured using QCM) of TL and BL system as a function of deposition unit. The TL system exhibits exponential growth, while BL system behavior remains linear.

higher linear growth, suggesting that the additional PAA layers were contributing to coating growth from the beginning of deposition. Above 5 deposition units the impact of the PAA layers was significantly more dramatic, resulting in a TL coating that was three times heavier than the BL coating at 14 deposition units (95 $\mu g/cm^2$ compared to 31 $\mu g/cm^2$).

This switch from linear to exponential growth by the addition of PAA is likely due to increased charged density resulting in faster diffusion of PEI and PAA across the monolayers.[9,24] Yang et al.[9] proposed that the exponential mass growth (25 to 320 $\mu g/cm^2$) of the 20BL PEI/PAA only films was due to the submersion of the PAA coating into the basic PEI solution causing an increase in PAA charge density, thus increasing the amount of PEI absorbed onto the substrate. The same phenomenon also occurred when the PEI coating was submerged in the acidic PAA solution. It was also reported that the fastest growth rate occurring at the same pH values was used in this study (10 for PEI and 4 for PAA).

For the same number of coating layers, Yang's 10BL pure polymer (PEI/PAA) coating is nearly three times heavier than the 10TL PEI/MMT/PAA coating reported here, suggesting that the MMT layer between the PEI and PAA may be limiting growth (150 $\mu g/cm^2$ and 52 $\mu g/cm^2$, respectively). For a similar quad layer coating (PEI/PAA/PEI/MMT), Podsiadlo et al.[24] previously reported that MMT layers had no impact on coating thickness growth and fluorescent labeled PAA and PEI diffused relatively unrestricted through the nanocomposite coating. At a six times higher concentration of MMT in the coating (10% compared to 64 ± 2%) and a fraction of the soaking time in the depositing solution (2 min compared to 1 min), the PAA has less time to diffuse across the significantly more concentrated/thicker MMT layers, which appears in this TL coating to be mitigating the accelerated growth due to a charge density increase that has been previously reported.

SEM images of the 20BL (Figure 2a,b) and 8TL (Figure 2c,d) coated PUF provided visual evidence of the coating quality (e.g.,

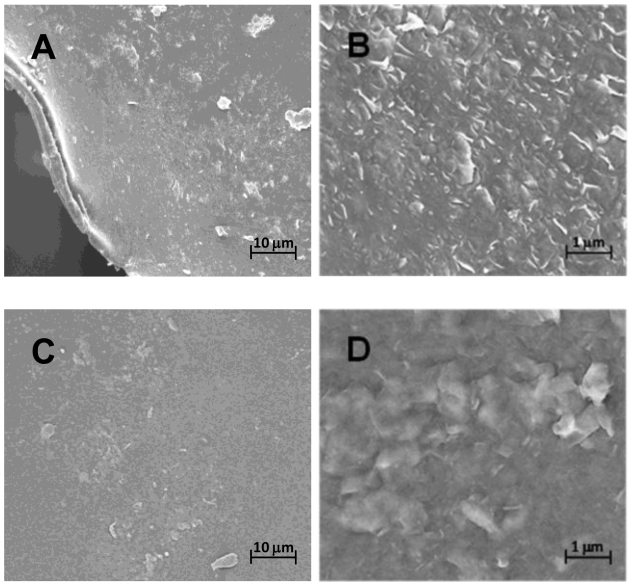

Figure 2. SEM image of 20BL coating at (A) 10 000× and (B) 100 000× and 8TL coating at (C) 10 000× and (D) 100 000× magnification.

extent of coating coverage and presence of MMT) and was used to measure coating thickness (Figure 3). At low magnification (Figure 2a) the MMT in the 20BL coating appeared uniformly distributed with some aggregations as large as tens of micrometers. The high magnification image (Figure 2b) revealed that, even though the MMT was distributed across the surface, some MMT sheets were only partially embedded in the PEI ,as evidenced by the sharp edges of the clay observed on the surface. The MMT was also well-distributed across the surface of the PUF in the 8TL coatings, but in contrast to the 20BL, the coating appeared much smoother as the last layer (PAA) was polymer and not clay. At low magnification (Figure 2c), the surface is featureless, suggesting that many regions do not contain MMT. However, high magnification (Figure 2d) reveals that these regions are completely covered with polymer embedded MMT.

Though the trends are aligned with the data in Figure 1, on the porous PUF the differences between the TL and the BL coatings were more significant. The 20BL coating had 1.6 times more monolayers than the 8TL coating (40 as compared to 24); however, the 8TL coating on PUF is nearly an order of

dx.doi.org/10.1021/mz300102h | ACS Macro Lett. 2012, 1, 820−824

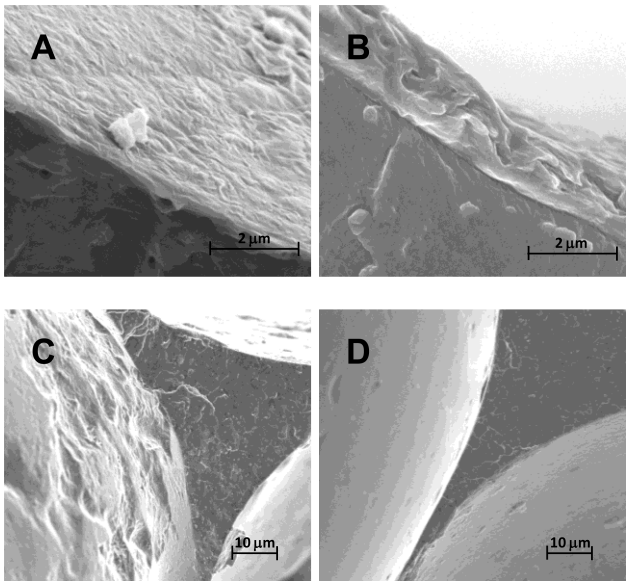

Figure 3. SEM images of a fracture edge of (A) 20BL coating at 100 000×, and 8TL coating at (B) 100 000×, (C) 10 000×, and (D) at 10 000× magnification. (C) and (D) are the images of single 8TL system in two different locations.

magnitude thicker than the 20BL coating (1000 ± 450 nm as compared to 122 ± 19 nm) (Figure 3a,b) and resulted in a five times heavier coating (0.60 ± 0.28% as compared to 3.18 ± 0.77% of the coated PUF mass). The higher absolute values measured on PUF is likely due to not drying the PUF specimens after each monolayer deposition[24] and the three-dimensional/porous structure of PUF reducing the washing efficiency. At least for the TL coatings, the less effective washing may be supported by the observed large morphology variations. The SEM images of two different locations on the same TL specimen show regions with large hills and valleys, creating thickness variations differing by almost 1 μm, and other regions that appear flat and homogeneous in comparison (Figure 3c,d).

The MMT concentration is the same for both the BL and the TL coatings (64 ± 2%, as measured by TGA). If the coating growth were purely due to the interaction of PEI and PAA (discussed above) then the MMT concentration would be relatively lower in the TL coatings. This suggests PAA is adhering to both the PEI and the MMT layers, which is resulting in the retention of MMT. Improved MMT retention was observed during the coating process, where for the BL the PEI wash solutions became cloudy from MMT release, but for the TL the PAA wash solutions remained clear throughout the coating process. The higher MMT loading and thicker coating achieved with the addition of PAA will be critical for the effectiveness of this intumescent fire retardant coating technology.

The cone calorimeter is a standard tool for measuring material flammability exposed to a constant external flux (e.g., ASTM E-1474). The test endeavors to represent how a sample would perform in an environment where other items are burning around the sample (rather than the sample being the only item burning). Typical values reported are the maximum (peak) heat released during test (PHRR), total heat release (THR, area under the curve), and time to ignition (tign, time to sustained ignition). The HRR data for the 8TL/PUF and uncoated PUF is provided in Table 1 and Figure 4. The 20BL/PUF and pure PUF results are indistinguishable (Table 1).

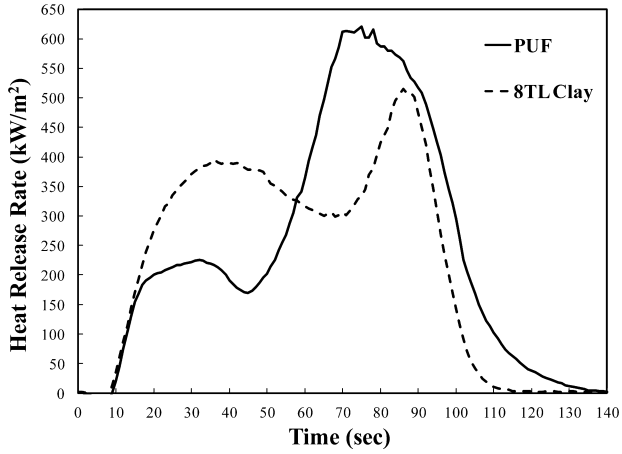

Figure 4. Heat release rate of untreated PUF and 8TL system per unit surface area in the cone as a function of burn time with an incident flux of 35 kW/m^2.

The HRR curves for 8TL MMT/PUF and PUF consist of two peaks, which represent the pyrolysis of isocyanate (first peak) and polyol (second peak).[26,27] The relative concentration of these polyurethane monomers is the same in both specimens, so the changes in peak characteristics suggest that the MMT coating has altered the pyrolysis process (this process change is currently under investigation). The reduction in PUF flammability due to the 8TL MMT-filled PUF coating is characterized by:

- 17% decrease in PHRR (critical value in accessing the flammability of a material),
- 15% increase in time to PHRR (related to escape time),
- 6% decrease in THR (related to the magnitude of fire threat), and
- 21% decrease in total burning time (related to how long a fire burns).

The flammability reduction caused by the 8TL coating is likely more significant than reported from the cone data because of PUF collapse and pool fire formation. The pure PUF collapses to form a pool of melted/degraded polyurethane during the test, whereas the 8TL coated PUF does not. In the cone, the collapsed PUF has a smaller surface area and is exposed to a lower heat flux because it is further from the cone heater. Both will result in

Table 1. Cone Calorimeter Results of Untreated PUF and 8TL System[a]

	peak 1		peak 2				
	HRR (kW/m^2)	time (s)	HRR (kW/m^2)	time (s)	THR (MJ/m^2)	residue mass %	burn time (s)
PUF	224 ± 12	32 ± 2	620 ± 26	75 ± 3	33 ± 2	2.2 ± 0.1	140 ± 2
20BL MMT/PUF	228 ± 15	33 ± 2	628 ± 20	72 ± 3	34 ± 2	2.2 ± 0.1	138 ± 2
8TL MMT/PUF	396 ± 15	36 ± 2	515 ± 15	86 ± 2	31 ± 2	2.6 ± 0.3	111 ± 2

[a]All values are reported with a 2σ uncertainty.

dx.doi.org/10.1021/mz300102h | ACS Macro Lett. 2012, 1, 820−824

lower HRR values.[26,28] In real fire, the melted pool is a pool fire that has been shown to typically increase the fire threat of soft furnishings by 35%.[29] The standard cone specimens and testing platform does not allow for this contribution to occur. Since the 8TL coating does not form a melt pool, an additional 35% reduction in PHRR could be measured in full-scale tests.

Compared to our previous CNF-filled LbL coating,[12] this MMT-filled analogue is not as effective of a fire-retarding system (MMT-filled has a 39% higher PHRR and 19% higher THR). However, the MMT coating reduction in PHRR is comparable to what is reported for commercial fire retardants,[12] may be a more environmental and health safety alternative, and may be used in lower concentrations.

In conclusion, the LbL TL approach (PEI/MMT/PAA) appears to a fast and effective route to fabricate high MMT-filled coatings on that significantly reduce PUF flammability. The PAA monolayers significantly impact MMT concentration and coating growth rate of PEI and MMT LbL coatings. The addition of PAA to a PEI/MMT BL coating causes a significant increase in the amount of coating deposited (five times heavier coating) while maintaining the same concentration of MMT within the coating (64 ± 2% MMT).

Since there is five times more coating mass, this TL (PEI/MMT/PAA) coating also results in five times more of the MMT fire retardant on the substrate. A faster and thicker coating has been demonstrated using a similar composition quad layer (PEI/MMT/PEI/PAA),[24] but the growth is dominated by the polymer interactions resulting in a MMT concentration that is 6.5 times less the TL coating and five times too low to be an effective fire retardant. The 8TL coating performed as well as many fire retardants already commercially used for PUF (e.g., 17% reduction in PHRR) and at lower loading levels.

Scheme 1. Illustration of Deposition Process for (a) 20BL and (b) 8TL Systems[a]

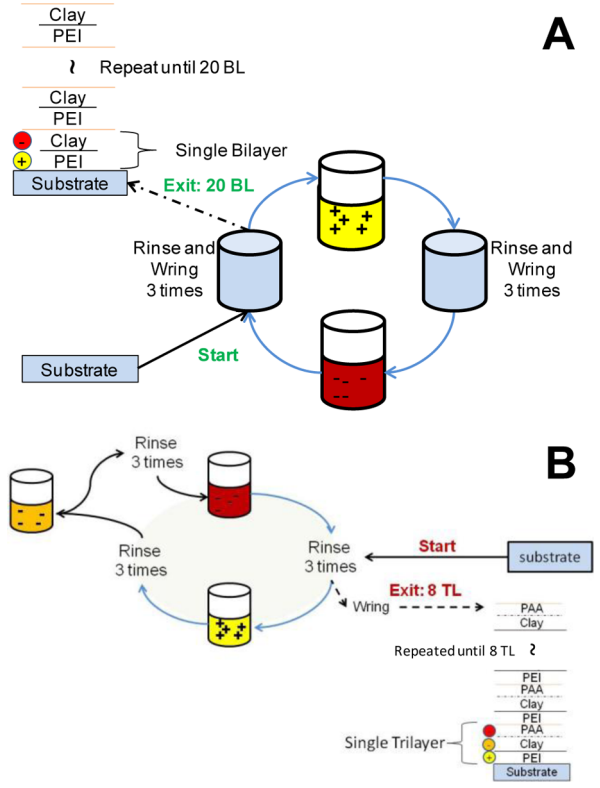

[a]The key difference between the two systems is the extra PAA layer between clay and PEI layers. After deposition, the specimen was dried in a convection oven for 12 h at 70 °C to remove excess water.

EXPERIMENTAL METHODS

Unless indicated otherwise, all values in the manuscript are reported with a 2σ uncertainty.

Certain commercial equipment, instruments, or materials are identified in this paper in order to specify the experimental procedure adequately. Such identification is not intended to imply recommendation or endorsement by the National Institute of Standards and Technology (NIST), nor is it intended to imply that the materials or equipment identified are necessarily the best available for this purpose. The policy of NIST is to use metric units of measurement in all its publications and to provide statements of uncertainty for all original measurements. In this document, however, data from organizations outside NIST are shown, which may include measurements in nonmetric units or measurements without uncertainty statements.

All materials were used as-received from the supplier unless otherwise indicated. Branched polyethylenimine (PEI, branched, M_w = 25 000 g/mol) and poly(acrylic acid) (PAA, M_w = 100 000 g/mol) were obtained from Sigma-Aldrich (Milwaukee, WI). Sodium montmorillonite clay (trade name is Cloisite Na+) was obtained from Southern Clay Products Inc. (Gonzales, TX). Standard (untreated) polyurethane foam (SPUF) was received from Future Foam Inc. (Fullerton, CA) and was stored as-received from the supplier. On the day of coating, nine substrates (length/width/height of 10.2 cm/10.2 cm/5.1 cm) were cut from a single substrate (length/width/height of 30.6 cm/30.6 cm/5.1 cm). Two polyelectrolyte solutions were prepared by dissolving 0.1 mass % PEI (cationic) and PAA (anionic) into deionized (DI) water and slowly agitating on a roller for 12 h. MMT suspension was prepared by adding 0.2 mass % MMT into deionized water and slowly agitating on a roller for 12 h.

Two different clay-filled LbL coatings were fabricated on the internal and external surfaces of the porous PUF (Scheme 1). The 20BL film was deposited by alternately submerging the PUF in the PEI solution (cationic), then in the MMT solution (anionic), and washing in DI water between each PEI or MMT monolayer deposition. This process was repeated 20 times to yield the clay-filled BL coating. The 8TL film was deposited using the same process except adding a submersion in the PAA solution (anionic) after depositing the MMT layer. This TL process was repeated 8 times. The final coatings were constructed of 20 PEI/MMT BLs and 8 PEI/MMT/PAA TLs. For both coatings, the initial submersion in PEI and MMT were 5 min, which was reduced to 1 min for each subsequent submersion in PEI, MMT, and PAA solutions. This longer initial submersion was necessary to improve durability of subsequent layers. A more detailed description of a LbL coating process has been previously published.[30]

A Q-sense E4 quartz crystal microbalance was used to measure the mass gain of each layer. A 5 MHz quartz crystal with gold was coated as described above. After each deposition, crystal was rinsed with deionized water and dried with N_2 gas. The mass of coatings on PUF was measured using a laboratory microbalance. The mass of clay was measured with a Q500 thermogravimetric analyzer (TGA, TA Instruments, New Castle, DE). TGA analysis was conducted on a 10 mg specimen at a linear heating rate of 10 °C/min to 800 °C under air. The clay mass % concentration was calculated from TGA and microbalance values. A Zeiss Ultra 60 field emission-scanning electron microscope (FE-SEM, Carl Zeiss Inc., Thornwood, NY) was used to acquire surface and cross-section images of the coatings on the PUF surface. All SEM samples were sputter-coated with 5 nm of Au/PD (60 mass %/40 mass %) prior to SEM imaging. The flammability assessment was based on results from a dual cone calorimeter (Fire Testing Technology, East Grinstead, United Kingdom), operating at 35 kW/m^2 with an exhaust flow of 24 L/s. The cone experiments were conducted according to standard testing procedures (ASTM E-1354-07), except that the pan sides were 1 cm tall and slightly flared away from the sample to allow all of the sides and the top surface to be exposed during the test.

dx.doi.org/10.1021/mz300102h | ACS Macro Lett. 2012, 1, 820−824

AUTHOR INFORMATION

Corresponding Author

*E-mail: rick.davis@nist.gov.

Notes

The authors declare no competing financial interest.

ACKNOWLEDGMENTS

The authors thank Alexander Morgan at University of Dayton Research Institute for cone calorimeter testing and Kirt Page for QCM measurements.

REFERENCES

(1) Decher, G. In *Multilayer Thin Films: Sequential Assembly of Nanocomposite Materials*; Decher, G., Schlenoff, J. B., Eds.; Wiley-VCH: Weinheim, Germany, 2003.

(2) Laschewsky, A.; Bertrand, P.; Jonas, A.; Legras, R. *Macromol. Rapid Commun.* **2000**, *21*, 319−348.

(3) Shimazaki, Y.; Nakamura, R.; Ito, S.; Yamamoto, M. *Langmuir* **2001**, *17*, 953−956.

(4) Sano, M.; Sato, M. *Langmuir* **2005**, *21*, 11490−11494.

(5) Lv, F.; Peng, Z. H.; Zhang, L. L.; Yao, L. S.; Liu, Y.; Xuan, L. *Liq. Cryst.* **2009**, *36*, 43−51.

(6) Bergbreiter, D. E.; Chance, B. S. *Macromolecules* **2007**, *40*, 5337−5343.

(7) Vossmeyer, T.; Schlicke, H.; Schroder, J. H.; Trebbin, M.; Petrov, A.; Ijeh, M.; Weller, H. *Nanotechnology* **2011**, 22.

(8) Sun, J. Q.; Zhang, L. B.; Li, Y.; Shen, J. C. *Langmuir* **2008**, *24*, 10851−10857.

(9) Yang, Y. H.; Haile, M.; Park, Y. T.; Malek, F. A.; Grunlan, J. C. *Macromolecules* **2011**, *44*, 1450−1459.

(10) Picart, C.; Boudou, T.; Crouzier, T.; Ren, K. F.; Blin, G. *Adv. Mater.* **2010**, *22*, 441−467.

(11) Su, P. G.; Shiu, C. C. *Sens. Actuators, B* **2011**, *157*, 275−281.

(12) Kim, Y. S.; Davis, R.; Cain, A. A.; Grunlan, J. C. *Polymer* **2011**, *52*, 2847−2855.

(13) Li, Y. C.; Schulz, J.; Mannen, S.; Delhom, C.; Condon, B.; Chang, S.; Zammarano, M.; Grunlan, J. C. *ACS Nano* **2010**, *4*, 3325−3337.

(14) Huang, G. B.; Zhu, B. C.; Shi, H. B. *J. Appl. Polym. Sci.* **2011**, *121*, 1285−1291.

(15) Gilman, J. W.; Bourbigot, S.; Shields, J. R.; Nyden, M.; Kashiwagi, T.; Davis, R. D.; Vanderhart, D. L.; Demory, W.; Wilkie, C. A.; Morgan, A. B.; Harris, J.; Lyon, R. E. *J. Mater. Sci.* **2003**, *38*, 4451−4460.

(16) Dubois, P.; Alexandre, M.; Beyer, G.; Henrist, C.; Cloots, R.; Rulmont, A.; Jerome, R. *Macromol. Rapid Commun.* **2001**, *22*, 643−646.

(17) Davis, R. D.; Gilman, J. W.; VanderHart, D. L. *Polym. Degrad. Stab.* **2003**, *79*, 111−121.

(18) Jiang, D. D. In *Fire Retardancy of Polymeric Materials*, 2nd ed.; Wilkie, C. A., Morgan, A. B., Eds.; Taylor and Francis: Boca Raton, FL, 2010; pp 261−299.

(19) Podsiadlo, P.; Kaushik, A. K.; Arruda, E. M.; Waas, A. M.; Shim, B. S.; Xu, J. D.; Nandivada, H.; Pumplin, B. G.; Lahann, J.; Ramamoorthy, A.; Kotov, N. A. *Science* **2007**, *318*, 80−83.

(20) Priolo, M. A.; Gamboa, D.; Holder, K. M.; Grunlan, J. C. *Nano Lett.* **2010**, *10*, 4970−4974.

(21) Yang, Y. H.; Malek, F. A.; Grunlan, J. C. *Ind. Eng. Chem. Res.* **2010**, *49*, 8501−8509.

(22) Elzbieciak, M.; Wodka, D.; Zapotoczny, S.; Nowak, P.; Warszynski, P. *Langmuir* **2010**, *26*, 277−283.

(23) Lutkenhaus, J. L.; Olivetti, E. A.; Verploegen, E. A.; Cord, B. M.; Sadoway, D. R.; Hammond, P. T. *Langmuir* **2007**, *23*, 8515−8521.

(24) Podsiadlo, P.; Michel, M.; Lee, J.; Verploegen, E.; Kam, N. W. S.; Ball, V.; Lee, J.; Qi, Y.; Hart, A. J.; Hammond, P. T.; Kotov, N. A. *Nano Lett.* **2008**, *8*, 1762−1770.

(25) Tran, N. H.; Dennis, G. R.; Milev, A. S.; Kannangara, G. S. K.; Wilson, M. A.; Lamb, R. N. *J. Colloid Interface Sci.* **2005**, *290*, 392−396.

(26) Kramer, R. H.; Zammarano, M.; Linteris, G. T.; Gedde, U. W.; Gilman, J. W. *Polym. Degrad. Stab.* **2010**, *95*, 1115−1122.

(27) Lefebvre, J.; Bastin, B.; Le Bras, M.; Duquesne, S.; Ritter, C.; Paleja, R.; Poutch, F. *Polym. Test.* **2004**, *23*, 281−290.

(28) Schartel, B.; Hull, T. R. *Fire Mater.* **2007**, *31*, 327−354.

(29) Pitts, W. M.; Hasapis, G.; Macatangga, P. Technical Meeting of Eastern States Section of the Combustion Institute; Eastern States Section of the Combustion Institute: College Park, MD, 2009.

(30) Davis, R. D.; Kim, Y. S.; Harris, R. H.; Nyden, M. R.; Uddin, N. M.; Thomas, T. *Exposure and Fire Hazard Assessment of Nanoparticles in Fire Safe Consumer Products: Interagency Agreement Final Report*; The National Institute of Standards and Technology: Gaithersburg, MD, 2011.